

# Advanced Modeling of Charge Trapping at Oxide Defects

F. Schanovsky, W. Goes, and T. Grasser  
Institute for Microelectronics, TU Wien  
Gußhausstraße 27-29/E360, 1040 Wien  
Fax: +43/1/58801-35099

**Abstract**—Several reliability issues in MOS transistors - such as the bias temperature instability, hot-carrier degradation, and gate leakage - have been indicated to involve the capture and emission of carriers at point-defects in the oxide. The trapping behavior of these defects depends on the device temperature and the oxide field in a highly non-trivial manner. Detailed capture and emission time constants of single defects have recently been obtained from time-dependent defect spectroscopy (TDDS) measurements. The complex behavior of these time constants is most accurately explained using a multi-state multi-phonon model. In this model, the defects capture and emit carriers through a non-radiative multi-phonon process. Additionally, each defect has (at least) two internal states where each of them gives rise to different trapping dynamics. We give a brief and hopefully intuitive introduction to the theory of non-radiative multi-phonon capture and emission and to the concept of multi-state defects. The relation to the commonly used Shockley-Read-Hall defect description in semiconductor device modeling is discussed.

## I. INTRODUCTION

The miniaturization of MOS transistors in the past decade has led to an increase in both the oxide field and the operation temperature, increasing the demands for stability of the insulating oxide. Additionally, the introduction of new materials into the production process results in more complex gate stacks. This increased complexity has brought along an increase in the number of defects in the insulating region, which severely affects the transfer characteristics of the transistor. In consequence, oxide-defect-based reliability issues such as the bias temperature instability (BTI), hot-carrier degradation (HCD), and stress-induced leakage currents (SILC) have climbed to the top of the list of reliability concerns for current technology nodes.

The explanation of the observed degradation effects and accurate life-time projections pose new challenges for semiconductor device simulators. Semiconductor device simulation is usually focused on defects in the semiconductor, which influence the charge transport in the device through scattering or recombination. The capture and emission of carriers at these defects is usually quite fast and the dependence of the capture rates on the applied voltage is largely determined by the carrier concentrations. Additionally, as the semiconducting material is usually crystalline, the defect sites are quite similar, which leads to a negligible variation in the capture and emission rates for different defects. Thus, a defect model based on average transition rates often gives a good description of the behavior of the defect ensemble.

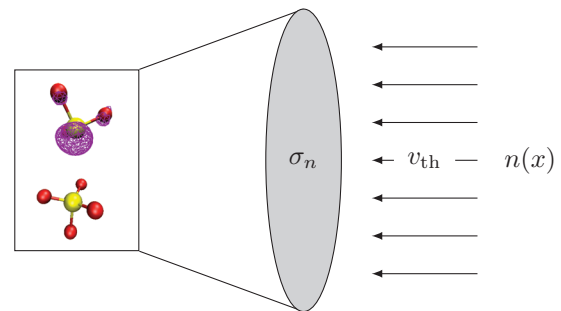


Fig. 1. In the Shockley-Read-Hall theory, the capture process is empirically described as a flux of particles through an opening of area  $\sigma$ . The particle flux is calculated by assuming that the carrier gas moves at the thermal velocity  $v_{th}$ .

For oxide defects, many of these simplifying conditions are not fulfilled. As the capture and emission processes are slower than in the bulk semiconductor, the charging and discharging kinetics need to be modeled more accurately. Additionally, the usually amorphous oxide makes every defect site unique and average descriptions give poor results. In the last years, a lot of information on the behavior of defects in the MOS oxide has been obtained from bias-temperature stress experiments [1]–[10]. The temperature and field activation observed in these experiments cannot be explained with standard defect models. Quite recently, the behavior of small-area transistors moved into the focus of the scientific attention. In these transistors, single charging and discharging events are visible as distinct steps in the drain current [7], [11]–[17]. The response of these small-area transistors to BT stress has revealed a quite complex behavior of the oxide defects, including a highly non-linear bias dependence of the time constants [18] and correlated gate and drain current fluctuations [19]–[22]. In the following we will focus on this recoverable component. The more permanent component is a topic of current research and the different explanations in the literature are still controversial [6], [8], [23], [24].

Thorough investigations of the experimental data have led to the development of a sophisticated defect model, which is able to explain most of the observed behavior. This defect model describes the carrier capture and emission as non-radiative multi-phonon transitions and also accounts for different internal states of the defect. This document outlines the basic properties of this multi-state multi-phonon defect

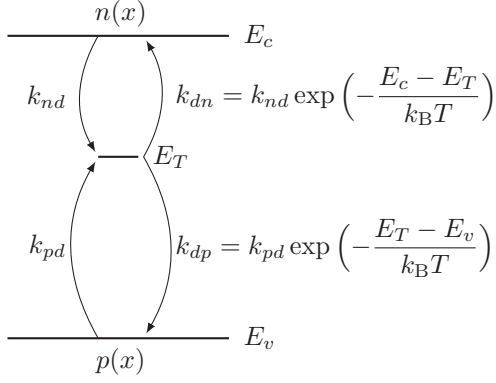


Fig. 2. The emission rates in the SRH model are calculated from the principle of detailed balance, which ensures that the occupancy of the defect in thermal equilibrium follows Fermi-Dirac statistics.

model, starting from the commonly employed Shockley-Read-Hall description of defects in semiconductors.

## II. DEFECTS IN SEMICONDUCTOR DEVICES

The Shockley-Read-Hall (SRH) theory put forward in 1952 [25] is the standard model for phonon-assisted recombination at defects in semiconductor devices. In the SRH model, the recombination center is described by a capture cross section  $\sigma$  and a trap level  $E_T$ . The defect is treated as a localized state that can either be occupied by an electron or unoccupied. The time evolution of the occupancy of the defect  $f$  is described as

$$\frac{\partial f}{\partial t} = -(k_{dn} + k_{pd})f + (k_{nd} + k_{dp})(1 - f), \quad (1)$$

where  $k_{nd}$  and  $k_{pd}$  are the rates for electron and hole capture (transition from the free state  $n$  or  $p$  to the localized state  $d$ ), and  $k_{dn}$  and  $k_{dp}$  are the rates for electron and hole emission (transition from the localized state  $d$  to the free state  $n$  or  $p$ ).

The capture process is modeled as a constant flux of the carrier gas moving at the thermal velocity  $v_{th}$  through an opening of area  $\sigma$ , see Fig. 1. The emission rates are derived from the principle of detailed balance [25], which ensures that in thermal equilibrium, the occupancy of the trap level follows Fermi-Dirac statistics for a state of energy  $E_T$ . The capture and emission rates in the SRH model read

$$k_{nd} = \sigma_n v_{th} n(x), \quad (2)$$

$$k_{pd} = \sigma_p v_{th} p(x), \quad (3)$$

$$k_{dn} = k_{nd} \exp\left(-\frac{E_c - E_T}{k_B T}\right), \quad (4)$$

$$k_{dp} = k_{pd} \exp\left(-\frac{E_T - E_v}{k_B T}\right), \quad (5)$$

see also Fig. 2.

In semiconductor device simulators, the SRH model is combined with a drift-diffusion based description of the carrier gas and an empirical parametrization for the defect centers using constant capture cross-sections and trap levels. While this description gives good results for the recombination at defects in the semiconductor bulk several works have shown

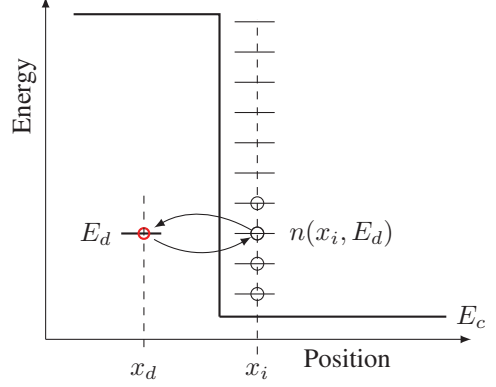


Fig. 3. In a simplified picture, the oxide defect gives rise to a localized state in the forbidden gap of the insulator. Charge carriers can enter this localized state through quantum mechanical tunneling.

that the detailed description of trapping kinetics requires a more sophisticated theory [26]–[28].

## III. PHONON-INDUCED TRANSITIONS

The physical process underlying thermally induced trapping is the non-radiative multi-phonon (NMP) transition. A quantum mechanical theory of NMP transitions was first published by Huang and Rhys in 1952 [29], which has since been broadly applied for the interpretation of measurement data of kinetic trapping experiments [30]–[33]. Introductions to multi-phonon transitions usually involve elaborate quantum mechanics and require a broad knowledge of physical chemistry and mathematical physics. In the present document we draw an intuitive picture for the special case of oxide defects, with the purpose of introducing the reader to the relevant concepts without going too much into the physical details. More detailed discussions can be found in the original papers [34], [35].

From the electronic structure point-of-view, an oxide defect gives rise to a localized state within the forbidden gap of the insulator, i.e. a state with limited spatial extent compared to the quasi-free states in the valence and the conduction band of the semiconductor. The charge carriers can enter or leave this state by means of quantum-mechanical tunneling. These tunneling transitions proceed elastically, i.e. the carrier neither loses nor gains energy in the process. As the energy of the orbit is sharply defined, only carriers which have the exact energy of the trap level can be trapped. Thus, as illustrated in Fig. 3, the trap level acts as an energetic selector and the capture rate will be

$$k_{nd} \propto T(E_d) D_n(x_i, E_d) f_n(x_i, E_d), \quad (6)$$

where  $T$  is a tunneling coefficient, and  $D_n$  and  $f_n$  are the local density of states and the occupation function for electrons. Similarly, the rate of emission from the localized state reads

$$k_{dn} \propto T(E_d) D_n(x_i, E_d) (1 - f_n(x_i, E_d)). \quad (7)$$

For the sake of simplicity, we introduce the density of occupied electron states  $n(x, E) = D_n(x, E) f_n(x, E)$  and write the

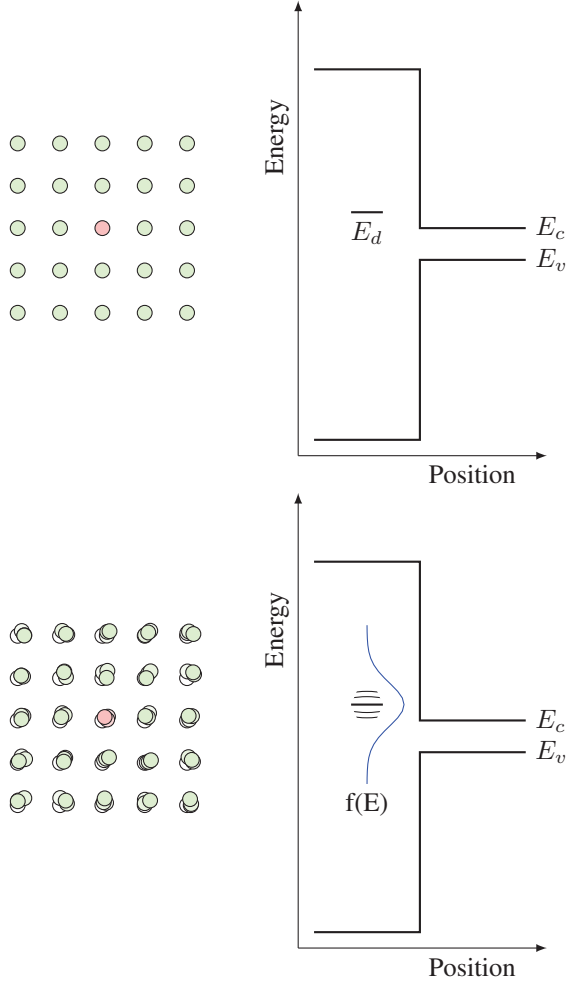


Fig. 4. The energetic position of the localized orbit depends on the instantaneous positions of the atoms in the defect structure. **(top)** At zero temperature the atoms rest at their equilibrium positions, and the energy of the localized orbit is sharply defined, as in Fig. 3. **(bottom)** At finite temperatures, the energy of the localized state will oscillate in a chaotic way due to the Brownian motion of the atoms. Thus, the sharp energy of the transition process has to be replaced by a statistical distribution.

capture and emission rates as

$$k_{nd} \propto T(E_d)n(x_i, E_d), \quad (8)$$

$$k_{dn} \propto T(E_d)(D_n(x_i, E_d) - n(x_i, E_d)). \quad (9)$$

This description assumes a classical carrier model, which does not account for quantum mechanical tunneling. In a quantum-mechanical carrier model, the tunneling coefficient is included in the densities which can then be evaluated at the defect site.

The energetic position of the localized electronic orbit depends on the electronic structure of the defect. According to the Born-Oppenheimer approximation, the electronic structure of any molecule depends on the position of its constituent atoms. For the trapping process, this implies that a well-defined level of the localized state can only be given at zero temperature, when the atoms are in their equilibrium position. At finite temperature, the atoms of the MOS device will exhibit a Brownian motion, randomly oscillating around their equilibrium position. This influences the defect level, which will also oscillate in an unpredictable fashion [36]. In

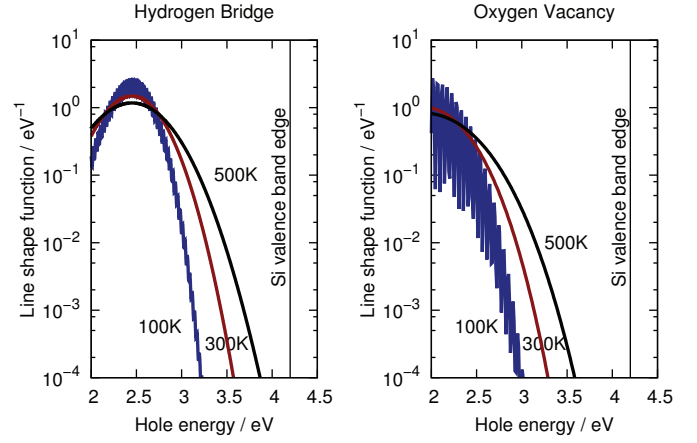


Fig. 5. Quantum mechanical line shapes calculated from atomistic defect models for three different temperatures. The 100K plots show oscillations due to the quantization of the atomic vibrations.

consequence, at finite temperatures the sharp energy level for the capture or emission transition is replaced by a probability density  $f(E)$  which gives the probability to find the level around a certain energy. This probability density is called *line shape* function, due to its origin in optical spectroscopy, where it describes the thermal broadening of absorption lines [29], [30]. Generally speaking, it needs to be considered that a change in the charge state of a defect changes its electronic structure and in consequence the equilibrium positions and oscillation frequencies. For this reason, the line shapes for capture and emission will be different. In consequence every charge transition has its own associated line shape. For this reason we indicate the initial charge state  $q_i$  and final charge state  $q_f$  for a line shape as  $f^{q_i/q_f}$ . For an acceptor-like defect, which is neutral when unoccupied and negatively charged when occupied by an electron, the NMP transition rates read

$$k_{nd} \propto \int_{-\infty}^{\infty} T(E)f^{0/-}(E)n(x_i, E)dE, \quad (10)$$

$$k_{dn} \propto \int_{-\infty}^{\infty} T(E)f^{-/0}(E)(D_n(x_i, E) - n(x_i, E)). \quad (11)$$

The line shapes of the defect may also reach out to the valence band of the semiconductor, making charge transitions by hole capture and emission possible. The rates for these transitions are analogous to their electron counterparts

$$k_{pd} \propto \int_{-\infty}^{\infty} T(E)f^{-/0}(E)p(x_i, E)dE, \quad (12)$$

$$k_{dp} \propto \int_{-\infty}^{\infty} T(E)f^{0/-}(E)(D_p(x_i, E) - p(x_i, E)). \quad (13)$$

The line shape functions is determined by the Born-Oppenheimer potentials of the defect in its various charge states [37]. The calculation of the line shapes requires to go into the details of the quantum-mechanical multi-phonon

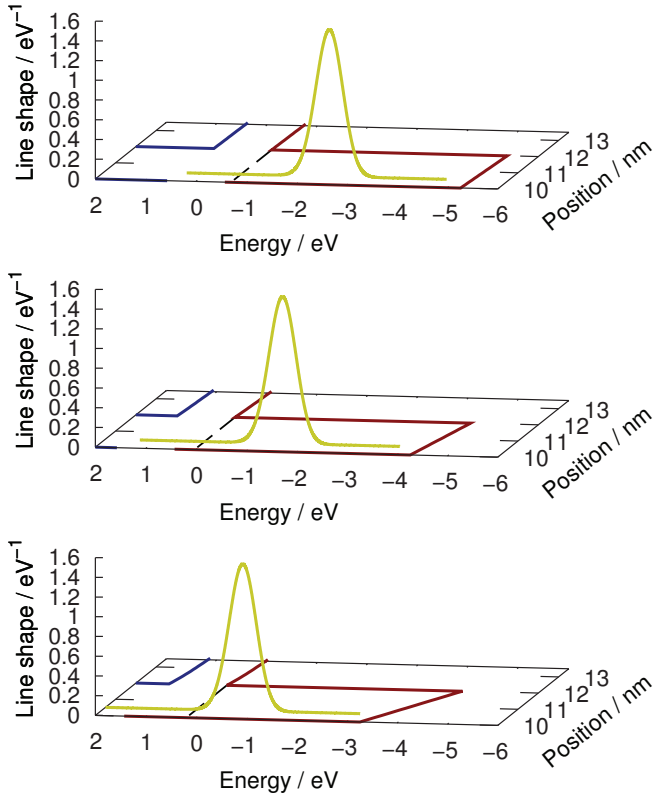


Fig. 6. The line shape is shifted by the electrostatic potential in the device. The figure shows the position of a line shape (yellow) relative to the valence band edge (red) and the conduction band edge (blue). Different gate bias voltages lead to different band bending and different positions of the capture line shape relative to the occupied charge carrier states. In the example, a negative bias shifts the line shape maximum closer to the occupied hole states near the silicon valence band edge. This increases the probability of a hole capture transition, which corresponds to the typical NBTI situation.

theory, which goes beyond the scope of this document. For all systems of practical interest the quantum-mechanical line shape cannot be calculated exactly due to the high dimensionality of the problem and the complexity of the Born-Oppenheimer potentials. It is thus common to assume parabolic potentials for the atoms in the different charge states of the defect. In this approximation, the atomic motion is described as a superposition of harmonic oscillations, which are called (local) eigenmodes of the vibration spectrum. Commonly it is further assumed that only a limited number (usually one) of these vibrational modes has an influence on the transition while the contribution of the other modes can be neglected. Analytical formulae are available for quantum-mechanical line shapes if the frequency of the relevant mode is not modified by the electronic transition [29], [30]. If the frequency changes, the quantum mechanical line shapes can still be calculated numerically [37], simple line shapes can also be calculated using classical statistical mechanics. These expressions neglect the quantum mechanical nature of the vibrating atoms, which is a reasonable for room temperature and above due to the large atomic mass [38].

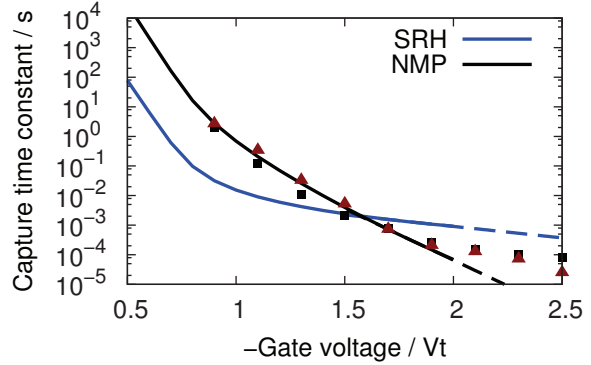


Fig. 7. Comparison of experimental capture time constants extracted from TDDS measurements to SRH and NMP. The SRH theory cannot properly explain the sharp decrease in the capture time constant at the onset of inversion. The NMP theory explains the strong bias dependence of the capture time constant very well between 0.8 V and 1.8 V. However, while the NMP time constant decreases exponentially for higher bias voltages, which is linear on the log scale, the experimentally observed time constants show some curvature.

#### A. The Trap Level in NMP Theory

While the capture cross-section of the SRH theory is clearly a construct of limited physical relevance, the trap level  $E_T$  can also be defined from the NMP theory. To do this, it is necessary to realize that the trap level of SRH theory does not refer to a quantum-mechanical level but a thermodynamical potential. This “thermodynamic” trap level [26], [32], [39], [40] is defined as the value of the electronic chemical potential (Fermi level) at which the defect changes its charge state in thermal equilibrium. For a donor-like trap this means if the Fermi level is below the trap level, the defect is dominantly in the positive state, while if the Fermi level is above the trap level, the defect is dominantly in the neutral state. Due to the differences in the electronic structure, the vibrational properties of the defect may vary strongly between the charge states. These differences add a change in entropy to the trap level, which is consequently slightly temperature dependent [26], [32].

#### B. Temperature and Field Activation

The NMP theory explains both the temperature and the field activation of the transition process which is experimentally observed. An increase in the temperature results in a broadening of the line shape, as shown in Fig. 5, which increases the capture probability the more, the further away the carrier energy is from the line shape maximum.

The field activation is stronger in oxide defects than in bulk defects due to the absence of free carriers. Just as for the valence and conduction band edges, the energetic position of the line shapes depends on the electrostatic potential in the device. Depending on the applied bias voltage, the electrostatic potential shifts the maximum of the line shape closer to or further away from the occupied states and thus increases or decreases the capture probability, see Fig. 6.

## IV. MULTI-STATE DEFECTS

Several experimental observations indicate the existence of internal defect states:

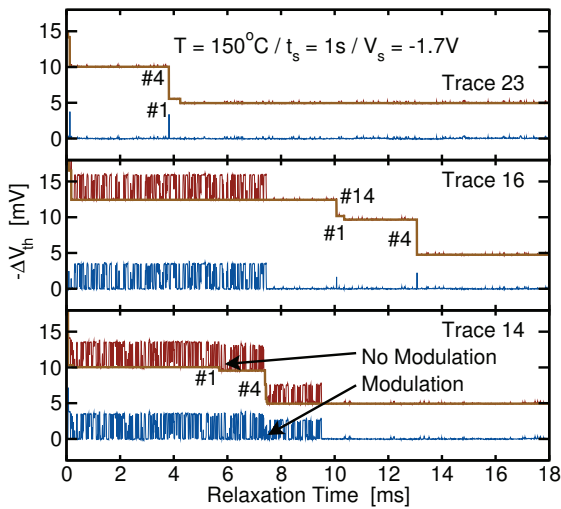


Fig. 8. In small-area MOS transistors, the charging and discharging transitions of oxide defects is visible as steps in the drain current. The recovery transients of these devices after bias-temperature stress usually shows the progressive discharging of the defect ensemble. However, in addition to the discrete recovery steps, the traces can also contain temporary RTN, which disappears after some time, see the three selected traces above. This behavior indicates the existence of multiple internal defect states with different trapping time constants.

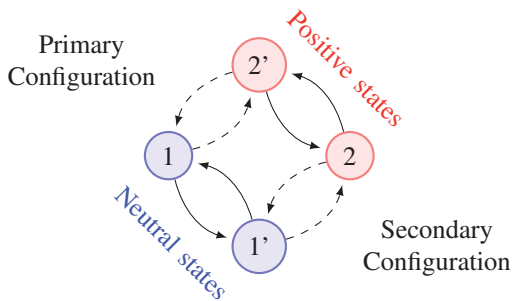


Fig. 9. In the multi-state multi-phonon model, an oxide defect has two stable structural configurations, which can assume a neutral and a positive charge state. The structural reconfigurations are barrier-hopping transitions ( $\rightarrow$ ) and the transitions between different charge states are non-radiative multi-phonon transitions ( $\dashrightarrow$ ).

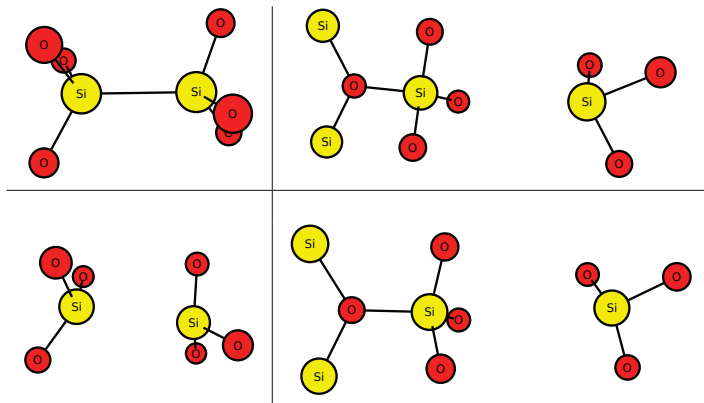


Fig. 10. The oxygen vacancy is a classical example for a bistable defect, which has two stable structural configurations. Structures of the dimer (left) and the puckered (right) configuration are shown for the neutral (top) as well as the positive (bottom) charge state.

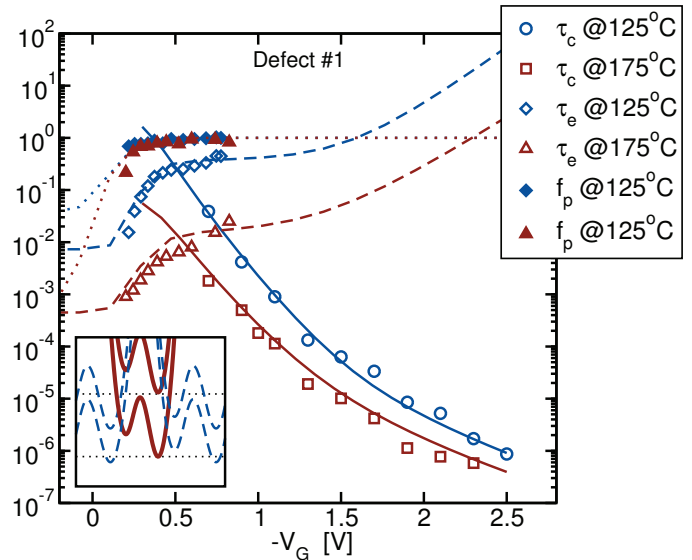


Fig. 11. In contrast to an NMP-only defect model, the multi-state multi-phonon model correctly gives the capture and emission time constants as observed in TDDS experiments. Excellent agreement is found for both the bias and the temperature dependence of the time constants. Taken from [7].

- **Decorrelation and bias frequency dependence of the capture and emission time constants.** A simple defect model which only switches between two charge states through an NMP process has an inherent correlation of the capture and emission time constants, which is in contrast to the experimental observations [18]. In addition, BT stress experiments with an AC stress voltage have found a frequency dependence of the capture time constant [41]. This frequency dependence is not explainable using a two-state defect but arises naturally from a multi-state defect model.
- **Curvature in the bias dependence.** The gate bias dependence of the capture time constants obtained from time-dependent defect spectroscopy (TDDS) measurements shows a curvature on the log scale in deep inversion, while NMP theory predicts an almost linear behavior in this regime, see Fig. 7 [7], [18].
- **Anomalous and temporary RTN.** In small-area transistors, the charging and discharging of defects is visible as steps in the drain current. The response of some of these defects following bias-temperature stress shows a temporary random-telegraph-noise signal which disappears after a while, see Fig. 8. This change in the trapping behavior of the defect is easily explained by different internal defect states with different capture and emission time constants.

All this behavior is well-explained by the multi-state multi-phonon model [7], [18], [42]. This model has been developed to explain the degradation and recovery behavior observed in bias temperature stress experiments, but has also been applied to random telegraph noise (RTN) and trap-assisted tunneling scenarios. As illustrated in Fig. 9, the model assumes that the oxide defects can exist in two charge states 1 and 2. In each charge state, the defect can assume one of two internal — or structural — states, which are denoted as 1 and 1' in

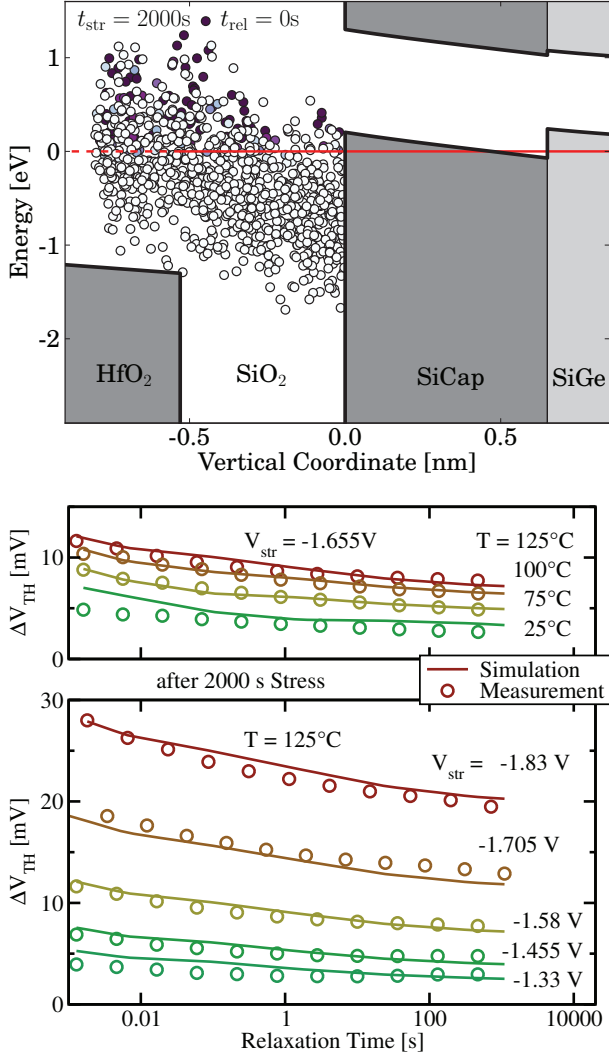


Fig. 12. Application of the multi-state multi-phonon model to BTI recovery in large-area MOS devices (taken from [43]). **(top)** A large enough ensemble of defects with varying parameters has to be produced to represent the defects in the MOS oxide. **(bottom)** Excellent agreement with the experimental data can be obtained from a careful calibration of the model.

charge state 1, and as 2 and 2' in charge state 2. It is generally assumed that 1 corresponds to a neutral charge state, and 2 to a positive charge state.

While the transitions between the charge states  $1 \rightleftharpoons 2'$  and  $2 \rightleftharpoons 1'$  are described using the NMP capture and emission rates (10)-(13), the transitions between the internal states  $1 \rightleftharpoons 1'$  and  $2 \rightleftharpoons 2'$  are described as an energetic barrier hopping transition using an Arrhenius law

$$k_{\alpha\beta} = \nu \exp\left(-\frac{E_{\alpha\beta}}{k_B T}\right), \quad (14)$$

with  $(\alpha, \beta) \in \{(1, 1'), (1', 1), (2, 2'), (2', 2)\}$  where  $\nu$  is the attempt frequency and  $E_a$  is the activation energy for the transition. The existence of internal defect states is a well-studied fact for different defects in SiO<sub>2</sub> [40], [44]–[49]. A classical example for a bistable defect as in the multi-state multi-phonon model is the oxygen vacancy in silicon dioxide [40], [50]. As shown in Fig. 10, this defect can exist in a dimer state, where the silicon atoms adjacent to the vacancy form a

bond. By overcoming an energetic barrier, which happens by chance through the random motion, one silicon atom can relax back and bond to a back-oxygen. This second configuration has different equilibrium energetics and oscillation frequencies and consequently different trapping behavior. Both of these bonding configurations can exist in both the neutral and the positive state. While the oxygen vacancy is usually taken as an example to illustrate the concept of a multi-state defect, the actual defect structure responsible for the experimentally observed degradation is still unknown and a topic of current research [50]–[55].

Once the states of the defect and the transition rates between those states are defined, the transient behavior of the defect can be modeled. While a two-state defect is fully described by a single occupancy function as in (1), a multi-state defect requires to assign a probability  $p_\alpha(t)$  for every state  $\alpha$  of the defect. These probabilities have to fulfill the condition  $\sum_\alpha p_\alpha(t) = 1$ . The time evolution of these probabilities is described by the master equation

$$\frac{\partial p_\alpha}{\partial t} = \sum_{\beta \neq \alpha} k_{\beta\alpha} p_\beta(t) - k_{\alpha\beta} p_\alpha(t). \quad (15)$$

As shown in Fig. 11, this multi-state model drastically improves the reproduction of the experimentally observed capture and emission time constants [7], [22], [42], [56]. Especially for the case of TDDS extracted effective capture and emission time constants, approximate expressions have been derived which represent the multi-state defect as an effective two-state defect.

For the description of the recoverable component of the BTI in large-area MOS devices an ensemble of defects with a random distribution of parameters for both the structural reconfiguration and the NMP transitions is generated. This defect ensemble must be large enough to capture the large variation of energy landscapes for the defects that arises from the amorphous nature of the MOS oxide. The degradation and recovery transients are then obtained from the integration of (15) for all the defects in the ensemble [5], [43], see Fig. 12.

## V. CONCLUSION

The modeling of the oxide defects involved in the reliability issues of modern MOS transistors such as the bias temperature instability, hot-carrier degradation and gate leakage requires a detailed description of the electrochemical reactions at the defect site. The recently developed multi-state multi-phonon model successfully reproduces a wide range of experimental data. We have given a brief introduction into the physical theory behind this defect model. The non-radiative multi-phonon theory, which describes the exchange of carriers between the defect and the rest of the device, as well as the concept of internal defect states have been introduced and compared to the standard Shockley-Read-Hall defect model. Examples have been given for the successful application of the model to experimental data.

## VI. ACKNOWLEDGEMENT

This work has received funding from the EC's FP7 grant agreement NMP.2010.2.5-1 (MORDRED).

## REFERENCES

- [1] D. Ang, S. Wang, and C. Ling, "Evidence of Two Distinct Degradation Mechanisms from Temperature Dependence of Negative Bias Stressing of the Ultrathin Gate p-MOSFET," *IEEE Electron Device Lett.*, vol. 26, no. 12, pp. 906–908, 2005.
- [2] V. Huard, M. Denais, and C. Parthasarathy, "NBTI Degradation: From Physical Mechanisms to Modelling," *Microelectronics Reliability*, vol. 46, no. 1, pp. 1–23, 2006.
- [3] S. Mahapatra *et al.*, "On the Physical Mechanism of NBTI in Silicon Oxynitride p-MOSFETs: Can Differences in Insulator Processing Conditions Resolve the Interface Trap Generation versus Hole Trapping Controversy?" in *Proc. Intl.Rel.Phys.Symp.*, 2007, pp. 1–9.
- [4] T. Aichinger, M. Nelhiebel, and T. Grasser, "Unambiguous Identification of the NBTI Recovery Mechanism using Ultra-Fast Temperature Changes," in *Proc. Intl.Rel.Phys.Symp.*, 2009, pp. 2–7.
- [5] T. Grasser *et al.*, "Understanding negative bias temperature instability in the context of hole trapping (Invited Paper)," *Microelectronic Engineering*, vol. 86, no. 79, pp. 1876–1882, 2009. [Online]. Available: <http://www.sciencedirect.com/science/article/pii/S0167931709002780>
- [6] V. Huard, "Two Independent Components Modeling for Negative Bias Temperature Instability," in *Proc. Intl.Rel.Phys.Symp.*, May 2010, pp. 33–42.
- [7] T. Grasser *et al.*, "The Time Dependent Defect Spectroscopy (TDDS) for the Characterization of the Bias Temperature Instability," in *Proc. Intl.Rel.Phys.Symp.*, 2010, pp. 16–25.
- [8] D. Ang *et al.*, "Reassessing the Mechanisms of Negative-Bias Temperature Instability by Repetitive Stress/Relaxation Experiments," *IEEE Trans.Dev.Mat.Rel.*, vol. 11, no. 1, pp. 19–34, 2011.
- [9] Y. Gao *et al.*, "On the Evolution of the Recoverable Component of the SiON, HfSiON and HfO<sub>2</sub> P-MOSFETs under Dynamic NBTI," in *Proc. Intl.Rel.Phys.Symp.*, Apr. 2011, pp. 935–940.
- [10] M. Duan *et al.*, "Defect Loss: A New Concept for Reliability of MOSFETs," *IEEE Electron Device Lett.*, vol. 33, no. 4, pp. 480–482, 2012.
- [11] V. Huard, C. Parthasarathy, and M. Denais, "Single-Hole Detrapping Events in pMOSFETs NBTI Degradation," in *Proc. Intl.Integrated Reliability Workshop*, 2005, pp. 5–9.
- [12] T. Wang *et al.*, "A Novel Transient Characterization Technique to Investigate Trap Properties in HfSiON Gate Dielectric MOSFETs — From Single Electron Emission to PBTI Recovery Transient," *IEEE Trans.Electron Devices*, vol. 53, no. 5, pp. 1073–1079, 2006.
- [13] H. Reisinger *et al.*, "The Statistical Analysis of Individual Defects constituting NBTI and its Implications for Modeling DC- and AC-Stress," in *Proc. Intl.Rel.Phys.Symp.*, 2010, pp. 7–15.
- [14] H. Reisinger *et al.*, "Understanding and Modeling AC BTI," in *Proc. Intl.Rel.Phys.Symp.*, 2011, pp. 597–604.
- [15] M. Toledano-Luque *et al.*, "Response of a Single Trap to AC Negative Bias Temperature Stress," in *Proc. Intl.Rel.Phys.Symp.*, 2011, pp. 364–371.
- [16] M. Toledano-Luque *et al.*, "Temperature Dependence of the Emission and Capture Times of SiON Individual Traps After Positive Bias Temperature Stress," *J.Vac.Sci.Technol.B*, vol. 29, pp. 01AA04–1–01AA04–5, 2011.
- [17] J. Zou *et al.*, "New Insights into AC RTN in Scaled High- $\kappa$ /Metal-gate MOSFETs under Digital Circuit Operations," in *IEEE Symposium on VLSI Technology Digest of Technical Papers*, 2012, pp. 139–140.
- [18] T. Grasser, "Stochastic Charge Trapping in Oxides: From Random Telegraph Noise to Bias Temperature Instabilities," *Microelectronics Reliability*, vol. 52, no. 1, pp. 39–70, 2012.
- [19] C. Chia-Yu *et al.*, "Correlation of Id- and Ig-Random Telegraph Noise to Positive Bias Temperature Instability in Scaled High- $\kappa$ /Metal Gate n-Type MOSFETs," in *Proc. Intl.Rel.Phys.Symp.*, 2011, pp. 3A.2.1–3A.2.6.
- [20] M. Toledano-Luque *et al.*, "Correlation of Single Trapping and Detrapping Effects in Drain and Gate Currents of Nanoscaled nFETs and pFETs," in *Proc. Intl.Rel.Phys.Symp.*, 2012.
- [21] B. Kaczer *et al.*, "Gate Current Random Telegraph Noise and Single Defect Conduction," *Microelectronic Engineering*, vol. 109, pp. 123–125, 2013.
- [22] W. Goes *et al.*, "A Comprehensive Model for Correlated Drain and Gate Current Fluctuations," in *Proc. Intl.Worksh.Comput.Electron.*, 2013, pp. 46–47.
- [23] T. Grasser *et al.*, "The 'Permanent' Component of NBTI: Composition and Annealing," in *Proc. Intl.Rel.Phys.Symp.*, April 2011, pp. 6A.2.1–6A.2.9.
- [24] S. Mahapatra *et al.*, "A Critical Re-evaluation of the Usefulness of R-D Framework in Predicting NBTI Stress and Recovery," in *Proc. Intl.Rel.Phys.Symp.*, April 2011, pp. 6A.3.1–6A.3.10.
- [25] W. Shockley and W. T. Read, "Statistics of the Recombinations of Holes and Electrons," *Phys. Rev.*, vol. 87, pp. 835–842, 1952.
- [26] O. Engström, "Influence of Entropy Properties on Measured Trap Energy Distributions at Insulator-Semiconductor Interfaces," *Appl.Phys.Lett.*, vol. 55, no. 1, pp. 47–49, 1989. [Online]. Available: <http://link.aip.org/link/?APL/55/47/1>
- [27] M. Kirton and M. Uren, "Capture and Emission Kinetics of Individual Si:SiO<sub>2</sub> Interface States," *Appl.Phys.Lett.*, vol. 48, pp. 1270–1272, 1986.
- [28] N. Zanolla *et al.*, "Measurement and Simulation of Gate Voltage Dependence of RTS Emission and Capture Time Constants in MOSFETs," in *Proc. Workshop on Ultimate Integration of Silicon*, Udine, Italy, March 2008, pp. 137–140.
- [29] K. Huang and A. Rhys, "Theory of Light Absorption and Non-Radiative Transitions in F-centers," *Proc. Roy. Soc. A*, vol. 204, pp. 406–423, 1950.
- [30] C. H. Henry and D. V. Lang, "Nonradiative Capture and Recombination by Multiphono Emission in GaAs and GaP," *Phys. Rev. B*, vol. 15, no. 15, pp. 989–1016, January 1977.
- [31] S. Makram-Ebeid and M. Lannoo, "Quantum Model for Phonon-Assisted Tunnel Ionization of Deep Levels in a Semiconductor," *Phys. Rev. B*, vol. 25, no. 10, pp. 6406–6424, May 1982.
- [32] O. Engstrom and H. G. Grimmeiss, "Vibronic States of Silicon-Silicon Dioxide Interface Traps," *Semicond.Sci.Technol.*, vol. 4, no. 12, p. 1106, 1989. [Online]. Available: <http://stacks.iop.org/0268-1242/4/i=12/a=012>
- [33] A. Palma *et al.*, "Quantum Two-Dimensional Calculation of Time Constants of Random Telegraph Signals in Metal-Oxide-Semiconductor Structures," *Phys. Rev. B*, vol. 56, no. 15, pp. 9565–9574, October 1997.
- [34] A. M. Stoneham, *Theory of Defects in Solids*. Oxford University Press, 1975.
- [35] A. M. Stoneham, "Non-Radiative Transitions in Semiconductors," *Rep.Prog.Phys.*, vol. 44, pp. 1251–1295, 1981.
- [36] V. Abakumov, V. Perel, and I. Yassievich, *Nonradiative Recombination in Semiconductors*. North-Holland, 1991.
- [37] F. Schanovsky, W. Goes, and T. Grasser, "An Advanced Description of Oxide Traps in MOS Transistors and its Relation to DFT," *J.Comp.Elect.*, vol. 9, pp. 135–140, 2010.
- [38] F. Schanovsky *et al.*, "A Multi Scale Modeling Approach to Non-Radiative Multi Phonon Transitions at Oxide Defects in MOS Structures," *J.Comp.Elect.*, vol. 11, pp. 218–224, 2012.
- [39] W. B. Fowler *et al.*, "Hysteresis and Franck-Condon relaxation in insulator-semiconductor tunneling," *Phys. Rev. B*, vol. 41, no. 12, pp. 8313–8317, 1990.
- [40] P. E. Blöchl, "First-principles calculations of defects in oxygen-deficient silica exposed to hydrogen," *Phys. Rev. B*, vol. 62, no. 10, pp. 6158–6178, September 2000.
- [41] T. Grasser *et al.*, "On the Microscopic Origin of the Frequency Dependence of Hole Trapping in pMOSFETs," in *Proc. Intl.Electron Devices Meeting*, 2012, pp. 470–473.
- [42] T. Grasser *et al.*, "Advanced Characterization of Oxide Traps: The Dynamic Time-Dependent Defect Spectroscopy," in *Proc. Intl.Rel.Phys.Symp.*, apr 2013, pp. 1–6.
- [43] P. Hehenberger *et al.*, "Quantum-Mechanical Modeling of NBTI in High- $\kappa$  SiGe MOSFETs," in *Proc. Simu.Semicond.Proc.Dev.*, 2011, pp. 11–14.
- [44] E. P. O'Reilly and J. Robertson, "Theory of Defects in Vitreous Silicon Dioxide," *Phys. Rev. B*, vol. 27, pp. 3780–3795, Mar 1983. [Online]. Available: <http://link.aps.org/doi/10.1103/PhysRevB.27.3780>
- [45] M. Boero *et al.*, "Structure and Hyperfine Parameters of E'<sub>1</sub> Centers in  $\alpha$ -Quartz and in Vitreous SiO<sub>2</sub>," *Phys. Rev. Lett.*, vol. 78, pp. 887–890, Feb 1997. [Online]. Available: <http://link.aps.org/doi/10.1103/PhysRevLett.78.887>
- [46] A. Yokozawa *et al.*, "Oxygen Vacancy With Large Lattice Distortion as an Origin of Leakage Currents in SiO<sub>2</sub>," in *Proc. Intl.Electron Devices Meeting*, December 1997, pp. 703–706.
- [47] N. Lopez, F. Illas, and G. Pacchioni, "Mechanisms of Proton Formation from Interaction of H<sub>2</sub> with E' and Oxygen Vacancy Centers in SiO<sub>2</sub>: Cluster Model Calculations," *J.Phys.Chem.B*, vol. 104, no. 23, pp. 5471–5477, 2000.
- [48] M. Busso *et al.*, "Ab Initio Simulation of the Oxygen Vacancy Bistability in Pure and Ge-Doped  $\alpha$ -Quartz," *Modelling and Simulation in Materials Science and Engineering*, vol. 10, no. 1, p. 21, 2002. [Online]. Available: <http://stacks.iop.org/0965-0393/10/i=1/a=303>
- [49] A. Kimmel *et al.*, "Positive and Negative Oxygen Vacancies in Amorphous Silica," *ECS Trans.*, vol. 19, pp. 3–17, 2009.

- [50] A. Leleis and T. Oldham, "Time Dependence of Switching Oxide Traps," *IEEE Trans.Nucl.Science*, vol. 41, no. 6, pp. 1835–1843, dec. 1994.
- [51] J. Conley Jr. *et al.*, "Electron Spin Resonance Evidence that  $E'_{\gamma}$  Centers can Behave as Switching Oxide Traps," *IEEE Trans.Nucl.Sci.*, vol. 42, no. 6, pp. 1744–1749, 1995.
- [52] J. Campbell *et al.*, "Atomic-Scale Defects Involved in the Negative-Bias Temperature Instability," *IEEE Trans.Dev.Mat.Rel.*, vol. 7, no. 4, pp. 540–557, 2007.
- [53] J. Ryan *et al.*, "Recovery-Free Electron Spin Resonance Observations of NBTI Degradation," in *Proc. Intl.Rel.Phys.Symp.*, 2010, pp. 43–49.
- [54] F. Schanovsky, O. Baumgartner, and T. Grasser, "Multi Scale Modeling of Multi Phonon Hole Capture in the Context of NBTI," in *Proc. Simu.Semicond.Proc.Dev.*, 2011, pp. 15–18.
- [55] F. Schanovsky *et al.*, "A Detailed Evaluation of Model Defects as Candidates for the Bias Temperature Instability," in *Proc. Simu.Semicond.Proc.Dev.*, 2013, accepted.
- [56] T. Grasser *et al.*, "On the Frequency Dependence of the Bias Temperature Instability," in *Proc. Intl.Rel.Phys.Symp.*, 2012, pp. XT.8.1–XT.8.7.